Solidification into undercooled succinonitrile and succinonitrile-acetone melts near and beyond the hypercooling limit

A. Schillings, A. Ludwig, P.R. Sahm, Gießerei-Institut der RWTH Aachen

1. Introduction

The following paper presents the investigations of rapid solidification processes into high undercooled melts of the plastic crystal succinonitrile (SCN) and the binary alloy succinonitrile-acetone (SCN-Ac). The main subjects of this paper are: (i) The kinetic attachment processes at undercoolings beyond the hypercooling limit of pure SCN are discussed with respect to the collision-limited growth model which is commonly used to describe solidification into undercooled metals. Especially solidification velocity measurements beyond hypercooling are a tremendous experimental challenge. Except our results presented here, data for only two other materials are available, namely Phosphorus [1] and the alloy system Co-Pd [2]. (ii) It is shown that complete solute trapping occurs during rapid solidification of SCN-Ac alloys. If the growth rate is high enough the solute pile up ahead of the solid-liquid interface vanishes and no solute partitioning takes place. In solidification experiments with metallic alloys this effect has already been proven [3].

The use of the plastic crystal SCN as basic material for the samples studied here is motivated by several reasons. The organic substances of the plastic crystal group exhibit a small entropy of fusion. Hence, they solidify with a non-faceted solid-liquid interface as is also common with metals. Plastic crystals are transparent materials and therefore solidification processes can be studied by means of optical methods. The thermophysical and thermodynamical properties of SCN and SCN-Ac are well known. Thus, the experimental results can be compared with theoretical predictions. Especially the circumstance that it was possible to achieve undercoolings up to and beyond the hypercooling limit of SCN [4, 5] is of major importance for the studies of rapid solidification phenomena.

2. Experimental

Thin capillaries made of borosilicate glass with an inner square cross section of (200×200) µm², a wall thickness of 100 µm and a length of 900 mm were filled with pure SCN or an SCN-Ac alloy. Prior to filling the as-delivered SCN material was zone-refined resulting in a purity level of 99.995 % or higher. The concentration of the different SCN-Ac alloys was estimated by measuring the liquidus temperature. The alloy concentration was then obtained by using the phase diagram reported by M.A. Chopra [6]. Three alloys of different concentrations were prepared: SCN-0.142 wt% Ac, SCN-0.196 wt% Ac and SCN-0.414 wt% Ac. Further details concerning the purification, sample preparation etc. can be found in [5].

The experimental set-up is shown in Fig. 1. The main parts are the heater, the cooler, the capillary filled with the sample material, an optical microscope with a video equipment and a device consisting of two photodiodes with an electronic amplifier circuit and a fast two-channel transient-recorder. The cooling device has two small entrance seals through which the capillary is introduced into the cooler. Within these seals small thermocouples and heat coils are integrated which allow to keep the substance in the capillary contained in the seals in the liquid state throughout the whole experiment. The part of the liquid sample positioned inside the cooler is therefore thermally isolated

from the outer parts. By reducing the temperature inside the cooler the liquid segment can be undercooled. As soon as a thermal steady state is established solidification is initiated by reducing the temperature in the right entrance seal. The solidification processes inside the capillary are observed by means of a microscope and a mounted CCD-camera connected to a video recorder.

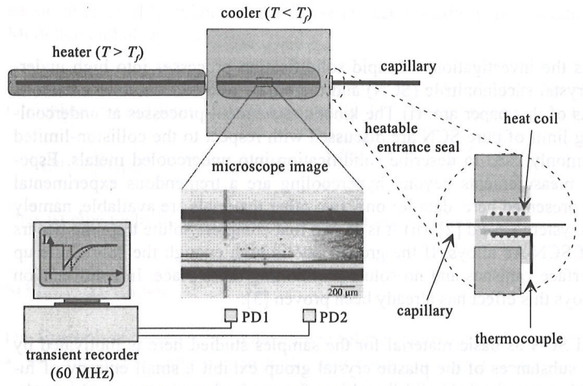

Figure 1: Scheme of the experimental set-up. The main parts are the heater, the cooler, the capillary, the transient recorder and the microscope(-picture). The magnified part on the right side shows the details of an entrance seal.

The solidification velocity is measured by the two independent photodiodes positioned in the light path of the microscope. Due to light scattering caused by a different refraction index of the solid and liquid phase the light intensity detected by the photodiodes decreases as soon as the solid-liquid interface passes the sensors. This change is registrated by the transient-recorder. From the time difference of the two recorded intensity signals and the lateral distance of the diodes the growth velocity of the solidifying material is calculated. More details are given in [5].

3. Results and Discussion

3.1 Rapid solidification into undercooled SCN

Observation of the solidification processes shows that the first solid growing into the undercooled melt is formed in direct contact to the glass walls of the capillary, Fig. 2. Thus the growth mode is termed "non-free". This primary two-dimensional surface layer is the starting point for the solidification perpendicular to the glass walls which is discussed elsewhere [5].

Fig. 3 presents the measured non-free growth velocities in dependence of the undercooling. Up to approximately 10 K the V-ΔT curve follows a power law. The slope of the subsequent linear increase of the velocity changes drastically when the undercooling exceeds the hypercooling limit. Following the LKT-theory [7] the net undercooling of the melt can be divided into a thermal undercooling ΔT_r, a capillary undercooling ΔT_R and a kinetic undercooling ΔT_k. The last term is important

during rapid solidification. As a first approximation it may be assumed that $\Delta T_k = V/\mu$ with the linear kinetic coefficient $\mu = f\cdot(\Delta h_f V_0)/(R_g \cdot T_f^2)$. Δh_f denotes the latent heat of fusion, V_0 the maximum growth rate, R_g the gas constant, T_f the melting point and f is a measure of the offered attachment sites at the solid-liquid interface.

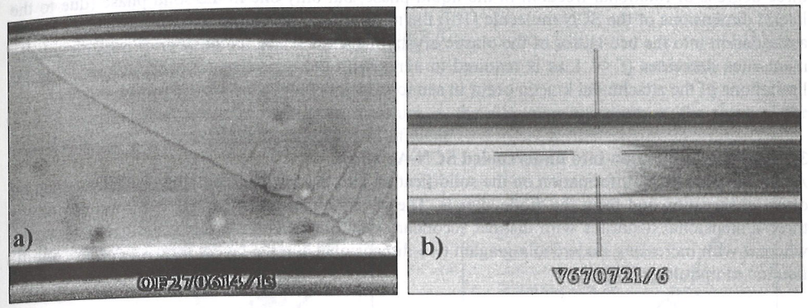

Figure 2: Surface structures observed during non-free growth into undercooled pure SCN. a) ΔT = 0.5 K, magnification: 250; b) ΔT = 13 K, magnification: 60.

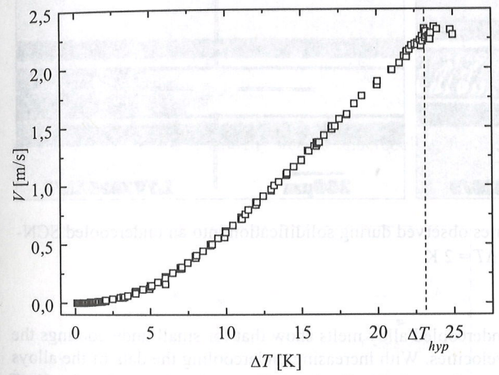

Figure 3: Solidification velocity versus undercooling of non-free growth. The velocity data beyond the hypercooling limit provide information on the linear kinetic coefficient.

As discussed in [5] the solid-liquid interface is almost planar during solidification at undercoolings larger than the hypercooling limit. Hence, $\Delta T_R \approx 0$ and the thermal undercooling is constant. The slope of the V-ΔT curve ($\Delta T > \Delta T_{hyp}$) then allows determination of the value $V_0 = (3.5 \pm 4.3)$ m/s. Examination of free growth data for pure SCN [8] results in $V_0 = 9$ m/s [9] which agrees well with our

non-free growth result for the attachment kinetic. The common assumption of a collision-limited growth ($V_0 = V_s$ = 1200 m/s, V_s: speed of sound in liquid SCN) with $f = 1$ is obviously not applicable to the solidification of the plastic crystal SCN. Either $f << 1$ has to be assumed or a diffusion-limited attachment occurs ($V_0 = V_D$, V_D is of the order of several m/s). Assuming a collision-limited growth the parameter f can be estimated to be 0.0075 for SCN. Since the SCN molecules exhibit three degrees of rotational freedom in the liquid phase, but only one in the solid phase (due to the lateral dimensions of the SCN molecule [10]) the molecules in the liquid have to reorientate before assimilation into the bcc-lattice of the plastic crystalline solid. Thus, the number of possible attachment sites decreases ($f << 1$ as is required to agree with the experimental observations). Similar limitations of the attachment kinetic occur in semiconductors (edgewise growth processes) [11].

3.2 Rapid solidification into undercooled SCN-Ac alloys

As for the pure SCN, information on the solidification into the undercooled alloy melts is gained by direct observation and from the diode signals. The observations show that for small undercoolings three-dimensional dendrites with distinct secondary dendrite arms grow along the capillary walls, whereas with increasing undercooling again two-dimensional surface layers form as primary solidification morphology (Fig. 4).

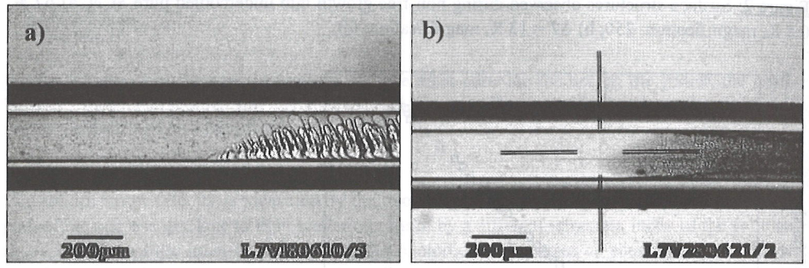

Figure 4: Primary solidification structures observed during solidification into an undercooled SCN-0.414 wt% Ac alloy. a) $\Delta T = 0.5$ K; b) $\Delta T = 2$ K.

The solidification velocities into the undercooled alloy melts show that for small undercoolings the values are comparable to free growth velocities. With increasing undercooling the data of the alloys approach the non-free growth velocities of pure SCN, Fig 5a. A linear plot shows that the V-ΔT curves of the different alloys and the curve of the pure SCN possess the same slope, Fig. 5b.

This overall behaviour is due to two effects. At small undercoolings a transition from a solute diffusion controlled growth to a thermal diffusion controlled growth takes place. This is accompanied with the circumstance, that for small undercoolings the solute diffusion process dominates the growth, leading to three-dimensional solute dendrites, as is observed. The influence of the glass is limited to the thermal diffusion process and is negligible in this case. On the other hand, with increasing undercooling the thermal diffusion increases in significance and therefore the presence of the glass results in a two-dimensional growth mode.

The second effect concerns the solute trapping occurring at high growth rates. Thermodynamic considerations of rapid growth phenomena show that the solidus temperature and the liquidus temperature are velocity dependent quantities, as well as the partition coefficient k, as is stated in the continuous growth model [12]. If complete solute trapping occurs ($k = 1$) the solidus and liquidus temperature coincide in the so-called T_0-temperature of the alloy ($T_{sol} = T_{liq} = T_0$). For dilute binary alloys W.J. Boettinger and S.R. Coriell [13] calculated the following expression (see Fig. 6):

$$T_0 = T_f + \frac{c_0 \cdot m_e \cdot \ln(k_e)}{k_e - 1} \qquad (1)$$

In this equation T_f denotes the melting temperature, c_0 the alloy concentration, m_e the slope of the liquidus line and k_e the equilibrium partition coefficient.

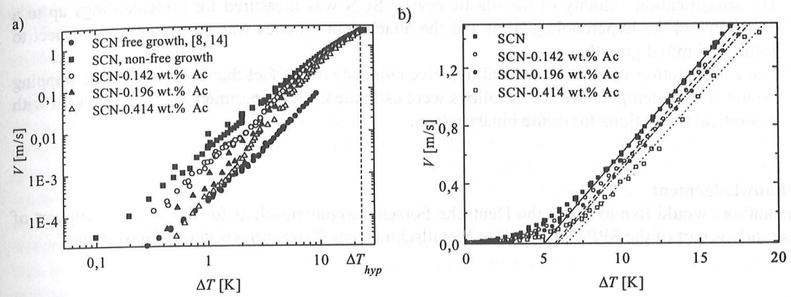

Figure 5: Solidification velocity versus undercooling for the different SCN-Ac alloys. a) log-log plot; b) linear plot.

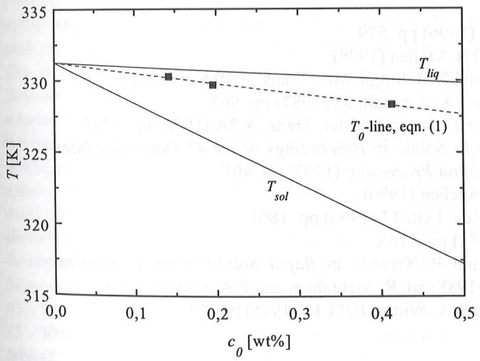

Figure 6: Phase diagram of the SCN-Ac system. The squares denote the experimental T_0-temperatures. The T_0-line is calculated using equation (1).

As an experimental temperature of reference to determine the undercooling of a melt the melting temperature T_f is used for pure SCN and the (equilibrium) liquidus temperature T_{liq} for the alloys (as was done in Fig. 5). Therefore, assuming complete solute trapping in the SCN-Ac alloys at high undercoolings, the shift in the velocity data away from the line fitted to the data of pure SCN demonstrates the temperature difference between the equilibrium liquidus temperature and the T_0-temperature of the corresponding alloy. From the data given in Fig. 5b one yields the T_0-temperatures presented as squares in the phase diagram of the SCN-Ac system (Fig. 6). These experimental data agree very well with the T_0-temperatures predicted by equation (1) for dilute binary alloys and thus support the interpretation of the occurrence of complete solute trapping in the SCN-Ac alloys.

4. Conclusions

The main results of the investigations presented in this paper can be summarised as follows:

- The solidification velocity of the plastic crystal SCN was measured for undercoolings up to a level beyond the hypercooling limit and the attachment kinetics was discussed with respect to collision-limited growth.
- The solidification velocities of the alloys give evidence to the fact that complete solute trapping occurs. The T_0-temperatures of the alloys were estimated. The experimental data agree well with theoretical predictions for dilute binary alloys.

Acknowledgement

The authors would like to thank the Deutsche Forschungsgemeinschaft for the financial support of this work as part of the SPP "Unterkühlte Metallschmelzen: Phasenselektion und Glasbildung".

Literature

[1] M.E. Glicksman and R.J. Schaefer, J. Crystal Growth **1** (1967) pp. 297
[2] T. Volkmann, G. Wilde, R. Willnecker and D.M. Herlach, J. Appl. Phys. **83** (1998) pp. 1
[3] K. Eckler, R.F. Cochrane, D.M. Herlach, B. Feuerbacher and M. Jurisch, Phys. Rev. B **54** (1992) pp. 5019
[4] A. Ludwig, Scripta Materialia **4** (1996) pp. 579
[5] A. Schillings, Dissertation, RWTH Aachen (1998)
[6] M.A. Chopra, M.E. Glicksman and N.B. Singh, Met. Trans. A **19A** (1988) pp. 3087
[7] R. Trivedi, J. Lipton and W. Kurz, Acta metall. **35** (1987) pp. 965
[8] M.E. Glicksman, R.J. Schaefer and J.D. Ayers, Met. Trans. A **7A** (1976) pp. 1747
[9] A. Schillings, A. Ludwig and P.R. Sahm, in *Proceedings of the 4th Decennial International Conference of Solidification Processing* (1997) pp. 401
[10] U. Lappe, Dissertation, RWTH Aachen (1990)
[11] D. Li and D.M. Herlach, Phys. Rev. Lett. **77** (1996) pp. 1801
[12] M.J. Aziz, J. Appl. Phys. **53** (1982) pp. 1158
[13] W.J. Boettinger, S.R. Coriell and R. Trivedi, in *Rapid Solidification Processing: Principles and Technologies II* (1988) ed. R. Mehrabian and P.A. Parrish, pp. 13
[14] M.E. Glicksman, M.B. Koss and E.A. Winsa, JOM **11** (1995) pp. 49